Level shifts, continuum lowering, and the mobility edge in dense plasmas

M. W. C. Dharma-wardana*
Institute of Theoretical Physics, University of California, Santa Barbara, California 93106
and National Research Council, Ottawa, Canada K1A 0R6†

François Perrot
Institute of Theoretical Physics, University of California, Santa Barbara, California 93106
and Centre d'Etudes de Limeil-Valenton, Boîte Postale 27, 94195 Villeneuve–Saint Georges CEDEX, France†

(Received 25 February 1991; revised manuscript received 31 October 1991)

The many-body problem in a hot dense plasma is treated using the "effective one-particle" description of density-functional theory. Three key ideas emerge, viz., (i) the neutral-pseudoatom (NPA) concept to describe a nucleus plus its electron distribution in the plasma, (ii) the concept of hopping electrons describing the effect of the ion-distribution on the electrons, which are shown to exist as bound, hopping, and free electrons, and (iii) the concept of the mobility edge replacing that of the continuum edge as we go to denser plasmas. The NPA concept shows that the electron-density profile around an ion in a plasma is very similar to that of the isolated neutral atom in a relevant configuration, and explains the absence of large polarization shifts predicted by simple plasma-screening theories. Several models of the ion distribution are used to study level shifts as a function of temperature and density. The change of continuum phase shifts with density is shown to give information about level formation. The appearance of hopping electrons signals the breakdown of Saha theory and the need to evaluate the effective charge Z^* of an ion in a dense plasma as a function of the ion distribution. The ion-correlation sphere is shown to be the "optimal volume" that maximizes the number of hopping states in the plasma. The mobility edge for the plasma percolation cluster is calculated and shown to depend on exchange-plus-correlation effects of electrons and ions, a Friedel-sum contribution, and a percolation contribution.

PACS number(s): 52.20.−j, 05.30.−d, 71.20.−b

I. INTRODUCTION

An important question that has been repeatedly raised [1–5] is the effect of the plasma environment on the bound electron levels of *an ion placed in a plasma.* The free-electron continuum is also changed by electronic and ionic correlation effects, leading to a modification of the density of states and a "lowering of the continuum edge." A knowledge of the bound energy levels, the density of states, other properties of the continuum, etc., is basic to microscopic calculations of plasma properties (e.g., plasma partition functions [6], ionization balance, electrical conductivity, opacities). Hence, any advance in our understanding of these matters is important.

Density-functional theory (DPT) provides a rigorous method for constructing effective one-body electron and ion equations leading to a set of "Kohn-Sham" (KS) eigenfunctions and eigenvalues for the electrons, and distribution functions for the ions. Here "pair interactions," etc., have been replaced by effective one-body interactions. But, as shown by the Hohenberg-Kohn-Mermin (HKM) theorems [7], *this is not an approximation.* However, the standard form of DFT is a static theory. Hence, while thermodynamics and static transport properties are rigorously given, dynamical properties require additional steps like the solution of the Dyson equation for the quasiparticle energies (see Ref. [8]). Nevertheless, in practice the KS equations give a good first approximation to the quasiparticle energies and eigenstates.

Here one may raise the question of ion and electron time scales. Since electrons are affected by the "instantaneous" ion distribution, which ion distribution should one use? For thermodynamics the *equilibrium* ion distribution is relevant, and it is this that is picked up by the HKM variational principle when applied to plasmas [8]. For other properties, the optimal distribution depends on the time scales involved and on the nature of the plasma. In many cases one may start from an equilibrium distribution and consider fluctuations about that distribution. This approach does *not* involve assumptions about the Born-Oppenheimer approximation or mean-field approximations to pair forces, etc., but merely a definition of an exact model for static properties, one that needs further theory (e.g., Dyson equation, or microfield theory, etc.) for handling time-scale effects. In this spirit a simple quasistatic theory of transient states (hopping electrons) will be discussed below.

The usual atomic-physics calculations for plasma do *not* invoke DFT. The ion distribution is replaced by, e.g., a single nucleus in a Wigner-Seitz (WS) cell (as in the $T=0$ ion distribution). Single-particle bound states in the cell are calculated using a one-body Schrödinger equation. The bound states have "average occupations" given by the Fermi distribution. The free electrons cannot be confined to a single cell and are roughly approximated by a Thomas-Fermi model. Rozsnyai's average-atom (AA) model (HOPE code) [9] is typical of such approaches. The Friedel-sum (FS) rule [10] is not satisfied in such models.

The theory is greatly improved if the ion distribution around the central nucleus is modeled so that there is no ambiguity in defining boundary conditions for the continuum states, permitting a full quantum treatment of the whole spectrum. Liberman's INFERNO models [11], and the model of Davis and Blaha [12] go in this direction. The DFT approach also yields a set of one-particle KS equations from which, by further approximation, these AA models can be derived. Further, the DFT model is constructed to give the correct Friedel sum. Chihara's "quantal hypernetted-chain" theory [13] also uses DFT within the language of the liquid-structure integral equations.

The objective of this paper is to relate the bound and free KS levels of an ion in a plasma to those of the isolated atom and the isolated ion, clarifying the nature of screening, ion correlations, and transient cluster structure in the plasma. The plan of the paper is as follows. We show in Sec. II that the electron-density profile $n(r)$ around an ion placed in a plasma is quantitatively almost equal to that of the corresponding neutral atom, establishing a charge-similarity principle (CSP). Thus, ions in plasmas are neutral pseudoatoms (NPS's), a concept first introduced explicitly by Ziman. This CSP clarifies the failure of Debye-Hückel, Thomas-Fermi, or hypernetted-chain descriptions of electron screening to the calculation of level shifts in plasmas, and why the expected "plasma-polarization shift" [1] of bound states is very small. The CSP is used in Sec. III to model plasma-level shifts. The density and temperature dependence of level shifts obtained from this CSP model (CSM) is compared with detailed DFT results. The breakdown of DFT at low densities due to the use of a single average configuration is discussed in Appendix B via a study of phase shifts and continuum resonances. In Sec. IV we introduce the concept of hopping electrons and discuss their role in the transition from strongly localized atomiclike states to fully delocalized continuum states. These hopping-electron states define a mobility edge fixing the onset of fully delocalized electron states. A combination of Lifchitz, Anderson, and Mott mechanisms [14,15] contributes to the mobility edge. Thus, we use the term "continuum edge" to define the onset of the continuous spectrum of a reference mean-field Schrödinger equation for Hartree electrons. This gets shifted due to electron and ion-correlation effects and exchange effects. We reserve the term "mobility edge" for that shifted continuum edge that includes the effect of percolation clusters arising from random ion-density fluctuation effects as well. In Sec. V the density of hopping states filling up the region between the last bound state and the continuum edge is calculated and compact expressions are given. The position of the shifted continuum edge is calculated as a sum of chemical-potential shifts, Friedel-sum contributions, and percolation-cluster effects. We present our summary and concluding remarks in Sec. VI.

II. MODELING AN ION IN A PLASMA

We consider, to be specific, an aluminum ion Al^{Z^*+} immersed in a plasma so that the nuclear charge $Z=13$, and the ionic charge is Z^*. In the following an energy level $i \equiv n,l$ in the plasma, in the isolated ion, and in the isolated atom will be denoted by ε_i^p, ε_i^i, and ε_i^a, respectively.

Hence we can define energy shifts referred to the isolated ion, or the isolated atom,

$$\Delta\varepsilon_i^{p-i}=\varepsilon_i^p-\varepsilon_i^i \ , \tag{2.1}$$

$$\Delta\varepsilon_i^{p-a}=\varepsilon_i^p-\varepsilon_i^a \ . \tag{2.2}$$

The isolated-atom or -ion energies ε_i^i and ε_i^a can be accurately calculated. Since an ion in a neutral plasma would be shown to behave as a NPA, the most useful reference will be the isolated atom. In Sec. II A we discuss the NPA model, in Sec. II B numerical results will be given, while in Sec. II C we comment on Debye-type linear screening models. In Sec. III we present a simple screening model arising from the results given in Sec. II C.

A. The neutral pseudoatom model

The calculation of the bound-state energies requires a proper description of the screening charge $n^p(r)$ in and around the ion in the plasma. This problem is equivalent to constructing a NPA in a solid and has been discussed at length in the theory of metals [16] by Ziman and others. The main idea is to construct a weak scatterer, essentially a neutral object whose Friedel sum [10] is zero, to which linear screening as well as the superposition principle can be applied. The NPA is not an "average atom," but for dense plasmas the most convenient analog of Ziman's NPA would be a "neutral average pseudoatom," and we will continue to call it a neutral pseudoatom for brevity and because the Friedel sum would be constructed as in Ziman, but adapted for the finite-temperature problem at hand. The correct calculation involves (i) a full quantum treatment of the continuum electrons so that the short-range correlations due to the internal structure of the ion, orthogonality, and Pauli exclusion are correctly treated, and (ii) inclusion of the effect of the ion-density distribution $\rho(r)$ around the ion under study. A common approximation for $\rho(r)$ is the "jellium model" of uniform density $\bar{\rho}$, in addition to the central nuclear charge. In simple NPA approaches a spherical cavity with a radius $r_{\rm WS}=(3/4\pi\bar{\rho})^{1/3}$ can be used to simulate the WS volume of exclusion of other ions by the central ion. The "ion plus its cavity" forms the NPA having a zero Friedel sum. In the plasma (or in fluids) such a volume of exclusion is naturally described [8] by the ion-ion-pair correlation function $g(r)$, which is related to the mean one-body ion distribution $\langle\rho(r)\rangle$ in the presence of the ion under study, placed at the origin. Thus

$$\langle\rho(r)\rangle=\bar{\rho}g(r) \ . \tag{2.3}$$

The use of (2.3) rather than the many-body instantaneous distribution $\rho(r_1,r_2,\ldots)$, where r_i refers to the instantaneous position of the ith ion, is an *approximation* if the object is to study short-time-scale phenomena. But the use of a one-body distribution is exact for static properties and is rigorous, as required by HKM theorems [7].

The systematic derivation of this model from the HKS variational principle is given in Ref. [8]. The stationary properties of the grand potential $\Omega[n,\rho]$ as a functional of the electron density $n(r)$ and the ion density $\rho(r)$, i.e., the properties $\delta\Omega/\delta n=0$ and $\delta\Omega/\delta\rho=0$, lead to two coupled equations, viz., a KS equation for the electrons and a Gibbs-Boltzmann equation for the ions. These are

$$\left[\frac{-\nabla^2}{2}+V_e(r)\right]\phi_i(r)=\varepsilon_i\phi_i(r)\ , \tag{2.4}$$

$$\rho(r)=\bar{\rho}\exp[-\beta V_i(r)]\ , \tag{2.5}$$

where the effective one-particle potentials $V_e(r)$ and $V_i(r)$ are of the form

$$V_e(r)=-\left[\frac{Z}{r}+V_p(r)\right]+V_{\rm xc}^e(r)+V_c^{ei}(r)\ , \tag{2.6}$$

$$V_i(r)=\bar{Z}\left[\frac{Z}{r}+V_p(r)\right]+V_c^i(r)+V_c^{ie}(r)\ . \tag{2.7}$$

No two-body potentials appear in these equations. It is emphasized that this not an approximation but a consequence of the HKM property that Ω is a functional of the time-averaged *one-body* densities, which are denoted for brevity by $n(r)$ and $\rho(r)$, without the usual averaging sign $\langle\ \rangle$. To reemphasize this point, if an instantaneous "snapshot" of the ion distribution is taken at some time instant t, then $\rho(r,t)=\sum_i\delta(\mathbf{r}-\mathbf{r}_i)$ where $\{\mathbf{r}_1,\ldots,\mathbf{r}_i,\ldots\}$ defines the instantaneous ion positions at time t. The "external potentials" of DFT, defined by (2.6) and (2.7) contain $V_p(r)$, which depends on the average distribution $\langle\rho(r)\rangle=\bar{\rho}g(r)$, as emphasized in Eq. (2.3), since the thermodynamic potential Ω depends only on the time-averaged distribution and not on the instantaneous distribution.

$\bar{Z}$ is an effective ionic charge for the "field ions." This arises from using the simplest example of a pseudopotential, viz., $\bar{Z}/r$, of zero well radius [17,18]. The many-body correlations and exchange effects are simulated by the one-body exchange-correlation (xc) potentials $V_{\rm xc}^e$, V_c^{ei}, V_c^{ie}, and V_c^i of DFT [19,20]. For example, if V_c^i is not retained the ion $g(r)$ does not show oscillations typical of strong-coupling correlations.

The Poisson potential V_p arising from the net charge density $\bar{Z}\rho(r)-n(r)$ also occurs in Eqs. (2.6) and (2.7). The densities $\rho(r)$ and $n(r)$ are determined self-consistently from (2.4) and (2.5). The electron density $n(r)$ is

$$\begin{aligned} &n(r)=n_b(r)+\Delta n(r)+\bar{n}\ ,\\ &n_b(r)=\sum_v n_i|\phi_i(r)|^2,\quad \varepsilon_i\le 0 \end{aligned} \tag{2.8}$$

where n_i is the Fermi function of the bound energy level i. The "displaced charge" of the continuum electrons $\Delta n(r)$ is

$$\Delta n(r)=2\sum_{l,k}(2l+1)n_k[|\phi_{kl}(r)|^2-|j_{kl}(r)|^2]\ ,$$

$$\varepsilon_k=k^2/2m$$

where $j_{kl}(r)$ is a spherical Bessel function. The continuum states ϕ_{kl} and energy ε_k carry phase shifts δ_{kl}. The self-consistent solution must satisfy the finite-temperature Friedel-sum rule and overall charge neutrality. The Friedel-sum rule controls the self-consistent interplay of bound, resonant, and free states (see Appendix B and Sec. IV).

If we had not started from the DFT variational principle we would have had to write Eq. (2.4) for each instantaneous ion configuration, and that too only as a mean-field (e.g., Hartree-Fock field) equation. On the other hand, Eqs. (2.4) and (2.5) are not mean-field equations, but proper many-body equations following from the properties $\delta\Omega/\delta n=0$ and $\delta\Omega/\delta\rho=0$ of the grand potential Ω. However, the KS eigenstates and the eigenvalues cannot be directly interpreted as *physical* one-particle energies, as given by the Dyson equation. (The same problem exists in commonly used AA models, irrespective of the model used for the ion distribution.) Further, in this model n and ρ have spherical symmetry, because they result from a double average, one on the electronic configurations and another on the ionic configurations, after having placed the nucleus to be studied at the origin. This ion at the origin is similar to an "impurity" embedded in an initially uniform system. Thus $n(r)=\bar{n}g_{ei}(r)$, where $g_{ei}(r)$ is the probability of finding an electron at the distance r from the central ion. This DFT treatment produces one-particle eigenstates that provide an exact treatment of the ion-ion and ion-electron distribution functions needed for thermodynamics, linear static transport coefficients, etc. It is clearly more useful than a table of eigenvalues and eigenfunctions obtained as a function of a very large number of arbitrary instantaneous ion configurations.

Equation (2.4) decouples from Eq. (2.5) under the weak-scatterer assumption. Then the screening distribution $n(q)$ is a superposition

$$n(q)=n^{(1)}(q)S(q)\ , \tag{2.9}$$

where $n^{(1)}(q)$ is the screening profile associated with a single ion. If the ion distribution could be frozen in a lattice, each ion occupies a Wigner-Seitz sphere and $\rho^{(1)}(r)=0$ for $r<r_{\rm WS}$ and $\rho^{(1)}(r)=\bar{\rho}$ for $r>r_{\rm WS}$. The total ion distribution $\rho(r)$ is also a superposition based on $S(q)$. The screening charge $n^{(1)}(r)$ associated with an ion placed in the cavity like ion distribution $\rho^{(1)}(r)$ can be calculated using the KS equation, and then the effect of the cavity can be subtracted off using perturbation theory. Where applicable this is simpler than solving the coupled equations (2.4) and (2.5). Perrot [16] has given calculations for liquid simple metals and plasmas using this approach to the NPA.

B. The position of the continuum edge

The bulk-plasma chemical potential is the zero of energy in these calculations, and defines the onset of the shifted continuous spectrum of the effective Schrödinger equation given by Eq. (2.4) containing exchange and correlation effects. The explicit shift in the electron chemical potential due to exchange-correlation interac-

tions is

$$\Delta\mu = \Delta\mu_{xc}(\bar{n}) + \Delta\mu_{ei}(\bar{\rho},\bar{n}) \ . \tag{2.10a}$$

$\Delta\mu_{xc}(\bar{n})$ is negative and is the *lowering of the continuum* due to exchange and correlation. The other term covers electron-ion-correlation effects [20]. The Debye-Hückel (DH) limit of μ_{xc} is $-k_{DH}/2$, where k_{DH} is the DH screening momentum. Evaluation of μ_{xc} for arbitrary degeneracies is given in Ref. [20]. An additional shift of the continuum arises from the presence of ions in the plasma that produce phase-shifted continuum states. Let N_0 be the integrated density of states in the absence of the ionic potential, which becomes N in the presence of an ion. Then, if $Z_F(k)$ denotes the Friedel sum [10], $\Delta N = N - N_0 = Z_F(k)$. The density of states $v_0(\varepsilon) = dN_0/d\varepsilon$. Hence $v_0(\varepsilon) \approx -\Delta N/\Delta\varepsilon$ and the energy shift per ion is

$$\Delta\varepsilon = -Z_F(k)/N_0 = -\pi^2 Z_F(k)/\vartheta k$$

where ϑ is the volume of the system. If N ions are added, and if the effect is taken to be additive (linear theory), the bottom of the continuum would be lowered by the amount

$$\Delta\varepsilon_{FS} = \lim_{k\to 0} -\bar{\rho}\pi^2 Z_F(k)/k \ . \tag{2.10b}$$

The finite-temperature phase shifts are known from the solutions of the plasma Kohn-Sham equation (2.4) and hence (2.10b) can be evaluated (note: AA models using a Thomas-Fermi continuum provide no phase shifts). An additional shift of the continuum edge (to give the mobility edge) will be discussed in Sec. V.

C. Numerical results from the neutral-pseudoatom model

In Fig. 1 we show as triangles the NPA calculation of the electron density $n^p(r)$ for an Al^{4+} ion in the plasma.

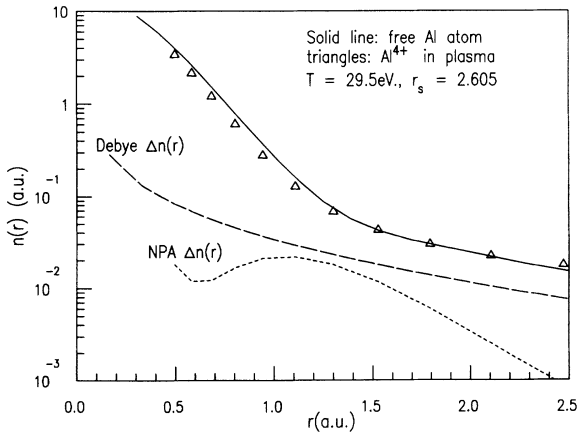

FIG. 1. Electron-density profile $n(r)$ in an isolated Al atom is shown (solid line) together with the $n(r) = n_b(r) + \Delta n(r) + \bar{n}$ at an Al^{+4} ion in a plasma (triangles) calculated from the Kohn-Sham equations (NPA model). The Debye-Hückel electron-density enhancement $\Delta n(r)$ should be compared with the $\Delta n(r)$ from NPA for the same ion. The plasma electron density $\bar{n} = 0.0135$ a.u. (9.1×10^{22} electrons/cm^3) and temperature is $4T_F$ (i.e., 29.53 eV). The shallowest "bound-state" energy is ≈ -0.843 eV ($3p$ state).

This $n^p(r)$ is made up of the bound charge $n_b^p(r)$ plus density displacement $\Delta n(r)$ plus uniform electron density $\bar{n}$. The NPA is calculated using the Kohn-Sham equations and taking the uniform ionic charge density outside the cavity to be $\bar{\rho}\bar{Z}$. We also show the NPA $\Delta n(r)$, the Debye $\Delta n(r)$, and the electron density in an isolated Al atom. The Debye $\Delta n(r)$ is for a point charge $\bar{Z}$ in jellium. The Debye $\Delta n(r)$ for the point charge in a cavity in jellium does not differ visually for r shown in Fig. 1. In Fig. 2 we give similar results for aluminum and carbon plasmas. It is evident that the Al ion or the C ion, together with their screening charges, look very much like the isolated atoms, except that in the isolated atom the electron density decays exponentially to zero, while in the plasma $n(r)$ drops towards the mean density $\bar{n}$. Instead of using a cavity, if the ion profile $\rho(r)$ were optimized using Eq. (2.7), the same conclusion regarding the similarity of the screening charges of isolated atoms and ions in plasmas would hold. We call this the "charge similarity principle" (CSP). This is mainly a result of the orthogonality of continuum states to core states, which strongly reduces the penetration of free electrons into the atomic-core region.

Figure 2 indicates that the continuum electrons associated with the Al pseudoatom manifest themselves as a deviation from the isolated atom electron-density profile for $r \geq 1.5$ a.u. This may well be taken as the size of the average atom, viz., r_a, in the plasma at this density and temperature. As the ionization is increased r_a shrinks, but the $n(r)$ for $r < r_a$ continues to obey the CSP.

D. Comment on linear-response models

The plasma effect is often treated by the Debye-Hückel or the Yukawa screening approach. Studies of plasma polarization shifts were motivated by the simple screening ideas that were current in the 1960's. But DH screening has been used even in recent plasma level-shift calculations [21]. It is currently used, without much discus-

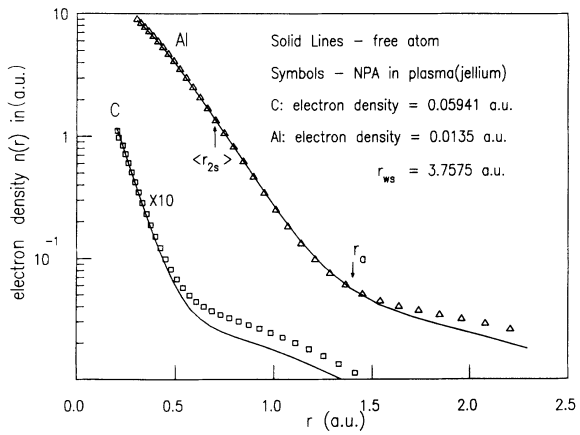

FIG. 2. Electron-density profiles $n(r)$ in isolated Al and C atoms are compared with the NPA density profiles for the Al and C ions placed in their respective plasmas. The Carbon $n(r)$ has been scaled down by 10. The nominal neutral-pseudoatom radius is r_a.

sion, even for very-dense-plasma microfields [22] and opacity calculations.

Although DH theory is applicable to the screening of two well-separated weak static charges, or a weak pseudopotential, it is inapplicable to ions with bound states, at length scales corresponding to the bound charge distribution, as seen from Figs. 1 and 2. Debye-Hückel, Thomas-Fermi, or classical hypernetted-chain (HNC)-type calculations [23] fail to describe screening electrons in the presence of bound electrons, not only because of the need to account for nonlinear effects, but also because the screening (i.e., "free") electron states have to be orthogonal to the core states. Average atom treatments where the core states are solutions of a Schrödinger equation while the continuum states are treated using a Thomas-Fermi approximation [9] also miss orthogonality corrections and are not trustworthy except in extreme conditions of temperature and (or) density.

In linear-response theory (LRT) the bare-electron–ion interaction (using $\hbar=e=m=1$ a.u.) given as $V_{ei}=-Z^*/r$ or as $V_{ei}(q)=-4\pi Z^*/q^2$ becomes the screened potential

$$V_{ei}^{p}(q)=V_{ei}(q)/\epsilon(q) , \tag{2.11a}$$

$$\epsilon(q)^{-1}=1+V_q\chi(q) . \tag{2.11b}$$

Here $\epsilon(q)$ is the plasma dielectric function, $\chi(q)$ is the electron-response function, while $V_q=4\pi/q^2$ is the bare Coulomb potential. If the small-q limit of the simplest model of $\chi(q)$ is used, then the screened potential becomes

$$V_{ei}^{p}(q)=-4\pi Z^*/(q^2+k_s^2) , \tag{2.12a}$$

where the square of the screening momentum k_s^2 is given by

$$k_s^2=k_{\rm TF}^2\int_0^\infty n_k\,dk . \tag{2.12b}$$

Here $k_{\rm TF}$, the Thomas-Fermi momentum $(4\alpha r_s/\pi)^{1/2}$, and k are in units of k_F, with $k_F=1/\alpha r_s$, $\alpha=(\frac{4}{9}\pi)^{1/3}$, and $r_s=(3/4\pi\bar{n})^{1/3}$. The Fermi function $n_k=[\exp\beta(E_Fk^2-\mu_e)+1]^{-1}$. The screening wave vector k_s^2 goes to $k_{\rm TF}^2$ or $k_{\rm DH}^2$ as $T\to 0$ or $T\to\infty$, respectively.

Consider the electron-density profile $n^p(r)$ formed around the ion in the plasma. We have, for DH,

$$V_{ei}^{p}(r)=-Z^*e^{-k_sr}/r \tag{2.13a}$$

and

$$n^p(r)=\bar{n}\exp[-\beta V_{ei}^{p}(r)] , \tag{2.13b}$$

$$\Delta n^p(r)=n^p(r)-\bar{n}\approx-\bar{n}\beta V_{ei}^{p}(r) . \tag{2.13c}$$

This DH profile $\Delta n(r)$ at an Al ion in a plasma is shown, together with that of the electron distribution $n(r)$ in an isolated Al atom in Fig. 1. The DH profile predicts a large (incorrect) charge pileup inside the atom. Also, the changes in the electron-ion interaction V_{ei}^{p} shifts the energy levels of the ion. From a first-order perturbation we have

$$\Delta\varepsilon_i^{p-i}=\langle\phi_i|Z^*[1-\exp(-k_sr)]r|\phi_i\rangle\simeq Z^*k_s . \tag{2.13d}$$

Instead of using perturbation theory, the Schrödinger equation with the DH potential [21] V_{ei}^{p}, or with a potential derived from an HNC calculation for the electrons [23] may be solved. Unfortunately, such calculations for level shifts miss the relevant physics.

III. SIMPLE APPROXIMATE FORMULAS FOR SCREENING AND LEVEL SHIFTS

The charge-similarity property CSP of the isolated atom and the plasma pseudoatom suggests that we may use the energy levels ε_i^i and ε_i^a for the isolated ion and the isolated atom to interpolate to the energy level of the plasma pseudoatom. Such a charge-similarity model (CSM) clarifies how energy levels are shifted by plasma effects and shell effects. We also compare three models where the plasma ions are modeled as a jellium, a jellium with a cavity, or by the self-consistent DFT distribution. We compare the trends in temperature and density obtained from the detailed DFT calculations with the predictions of the present CSM. In Appendix A we develop simple formulas that can often be used without the perils of DH theory.

Let i,j denote bound levels ($\equiv n,l$) while the "free"-electron states k,l (the continuum) are collectively treated as a "shell" denoted by f. In the NPA model the free electron shell f is largely outside the atom for $r\geq r_a$. The electron occupation number of the level i is n_i, while n_f denotes the number of free electrons in the NPA, i.e., on integrating over $r\geq r_a$.

The energy of the ith level of an ion in a plasma can be written as

$$\varepsilon_i^p\approx\varepsilon_i^a+\langle\phi_i^a|\Delta V_c^{p-a}+\Delta V_{\rm xc}^{p-a}|\phi_i^a\rangle . \tag{3.1}$$

The Coulomb term ΔV_c^{p-a} is

$$\Delta V_c^{p-a}=\sum_j{}'\int d\mathbf{r}'[n_j^p(r')-n_j^a(r')]\Big/|\mathbf{r}-\mathbf{r}'| . \tag{3.2}$$

The primed summation implies $j\neq i$. The exchange-correlation correction (correct to first order in δn) has the form

$$\Delta V_{\rm xc}^{p-a}=\sum_j{}'\int d\mathbf{r}[n_j^p(r)-n_j^a(r)]\delta V_{\rm xc}^{ee}(n)\Big/\delta n(r) , \tag{3.3}$$

where $V_{\rm xc}^{ee}(n)$ is the Kohn-Sham exchange-correlation potential at temperature T. The ion-electron and ion-ion correlation potentials V_c^{ie} and V_c^{i} also contribute in the same way but we disregard them in this discussion. For $j=f$, i.e., for the free-electron density $n_f^p(r)$, the atomic term $n_f^a(r)$ is zero but, because of the neutralizing charge density of the ionic background we use $\Delta n_f^p(r)=[n_f^p(r)-\bar{n}g(r)]$ instead of $n_f^p(r)$ in (3.3). Hence we write (3.1) as

$$\varepsilon_i^p=\varepsilon_i^a+\sum_j{}'V_{ij}[n_j^p-n_j^a]+\langle V_{if}\Delta n_f^p\rangle , \tag{3.4}$$

where the free-electron term $j=f$ is given as the last term. The "matrix elements" V_{ij} in (3.4) contain electrostatic and exchange-correlation contributions (in a DFT sense). The level shift arises from the discrete levels j as well as the plasma effect term $j=f$. When the ion is

TABLE I. Kohn-Sham eigenvalues for Al^{Z^*+} ions in their ground state in free space. Only occupied states are given. The energies are in hartrees and are negative. An exchange-correlation correction in LDA has been included.

Z^* Level	0	1	2	3	4	5
1s	55.168 19	50.481 23	55.945 66	56.474 12	58.082 22	59.866 17
2s	3.935 36	4.242 615	4.693 08	5.201 24	6.433 66	7.758 11
2p	2.564 42	2.872 10	3.322 54	3.830 37	5.096 99	6.473 86
3s	0.286 45	0.546 65	0.877 24			
3p	0.102 24					

placed in a plasma, the main effect is to change the n_j while the matrix elements V_{ij} remain more or less unchanged. These matrix elements can be evaluated from the energies ε_i^i and ε_i^a of the isolated ionic species and the isolated atom, respectively. Such a set of energies for Al is given in Table I. Tables II and III give results of KS energy-level calculations for plasmas and provide a means of testing the model (CSM) presented here. This model is in many ways similar to the "inner-screening–outer-screening buildup" model discussed by More [24], where the level energies are taken as simple functions of the level populations.

As a specific example let us consider the energy level 2s of a once ionized Al species, viz., Al^{1+} in a plasma (e.g., at density=0.008 437 5 a.u., i.e., $\frac{1}{32}$ of the normal density, see Table II for DFT results). Taking the isolated atom as the reference we can write, from (3.4),

$$\varepsilon_{2s}^p = \varepsilon_{2s}^a + V_{2s,3s}(n_{3s}^p - n_{3s}^a) + V_{2s,3p}(n_{3p}^p - n_{3p}^a) + \langle V_{2s,f}\Delta n_f^p \rangle \ . \tag{3.5}$$

The principle plasma effect is found in the last term and we concentrate on that. The 2s electron is practically *inside* the atom, i.e., $r_{2s} < r_a$, and $V_{2s,f}$ is just the Coulomb interaction $1/r$. Hence the last term of (3.5) is

$$\langle V_{2s,f}\Delta n_f^p \rangle \approx \int_{r_a}^{\infty} \Delta n_f^p(r')4\pi r'^2 dr'/r' \ . \tag{3.6}$$

Unlike DH theory, here the charge pileup interacts with the *electron* in the *i*th level and does not directly screen the electron-nuclear interaction since the charge pileup (see Fig. 1) close to the nucleus is small due to orthogonality and other quantum effects responsible for CSP. The density and temperature dependence of the level shift implied by (3.6) is more complicated than from DH theory, which gave in Eq. (2.13d) a linear dependence in $k_s Z^*$. Appendix A shows that the shift could be proportional to the k_s^2, Eq. (2.12b), or to a higher power. In Fig. 3 we plot the DFT-calculated plasma-atom energy shifts $\Delta\varepsilon^{p-a}i = \varepsilon_i^p - \varepsilon_i^a$ for several *i*, as a function of k_s^2, for several plasmas (some of the data are in Tables II and III). The k_s^2 dependence expected from CSM is seen in Fig. 3(a) where the results of DFT energy-level shifts for the Al and Ca plasmas are displayed. At $T=0$ the k_s^2 dependence implies an $\bar{n}^{1/3}$ dependence on the density. In the classical limit this becomes $\bar{n}/T$, whereas the behavior at finite temperature given by DFT is more complicated. Figure 3(b) shows the temperature dependence at a fixed density for the 3s-Ca level and the 2s-carbon level. Clearly the simple theory is useless for the Ca-3s

TABLE II. Kohn-Sham energy levels (hartrees) of An Al-ion placed in a plasma modeled by jellium (*J*) or jellium with a cavity (*C*). The electron density is 0.000 843 7a.u. ($\sim 5.69\times10^{21}$ e/cm^3), i.e., $r_s=6.565$ a.u. The energy ε_{nlm}, Fermi occupation factor f_{nlm}, and the orbital radius $\langle r_{nlm} \rangle$ are given where relevant. The Fermi temperature $T_F=1.16$ eV (=0.0426 hartrees).

	$T=0$		$T=2T_F$	$T=4T_F$
	C	*J*	*J*	*J*
$-\varepsilon_{2s}$	3.7685	3.7493	3.8591	4.0674
$-\varepsilon_{2p}$	2.3975	2.3781	2.4879	2.6962
$-\varepsilon_{3s}$	0.120 61	0.115 42	0.198 51	0.338 32
f_{3s}	1.0	1.0	0.7505	0.4132
$\langle r \rangle$	2.619	2.692	2.550	2.380
$-\varepsilon_{3p}$			0.018 80	0.130 52
f_{3p}			0.2677	0.1727
$\langle r \rangle$			3.973	3.012
$-\varepsilon_{4s}$				0.004 04
f_{4s}				0.090 54
$\langle r \rangle$				11.566

TABLE III. Comparison of energy levels (hartrees) from three models of the ion distribution (a) jellium, (b) self-consistent spherically averaged ion profile $\bar{\rho}g(r)$, and (c) jellium with a cavity of radius r_{WS}. The calculations are at $\bar{n}=0.0135$ a.u., i.e., 9.11×10^{22} e/cm^3.

	$T=T_F$ (7.38 eV)=0.2712 a.u. $\mu=-0.005\,65$ a.u., $\mu_{xc}=-0.261\,87$ a.u.			$T=2T_F$ $\mu=-0.667\,30$ a.u., $\mu_{xc}=-0.230\,145$ a.u.		
Level	Jellium	Profile	Cavity	Jellium	Profile	Cavity
$1s$	−54.876	−54.801	−54.765	−55.219	−55.137	−55.079
$2s$	−3.660 92	−3.5752	−3.5275	−3.9331	−3.8318	−3.7554
$2p$	−2.288 85	−2.2039	−2.1564	−2.5659	−2.4661	−2.3906
$3s$	−0.081 98	−0.046 48		−0.185 79	−0.1123	
$3p$				−0.008 975		
$\bar{Z}$	2.0485	2.2030	3.002 18	1.4321	2.7969	3.2470

level. When a fully self-consistent ion profile is included [in the sense of the DFT equations (2.4)–(2.7)] the results are intermediate between those of jellium and cavity models (see Table III). As seen in Fig. 3(a), the linear behavior breaks down for low densities ($k_s^2\to0$ limit) even for the $T=0$ limit. The data in Figs. 3(a) and 3(b) do not give a zero shift in the $k_s^2\to0$ limit. We discuss this case in detail in Appendix B, as it brings out the role of continuum resonances, etc., in determining level formation.

IV. HOPPING ELECTRONS AND QUASILOCALIZED STATES

Solution of the Kohn-Sham equations for the ion-profile model [cf. Eqs. (2.4)–(2.7)] provide KS eigenstates for the charge-neutral ion-electron system contained in the correlation sphere (radius $R_g\approx10r_{WS}$), consisting of the central nucleus and a spherically averaged cluster of some 1000 plasma ions. Three types of electron eigenfunctions are obtained.

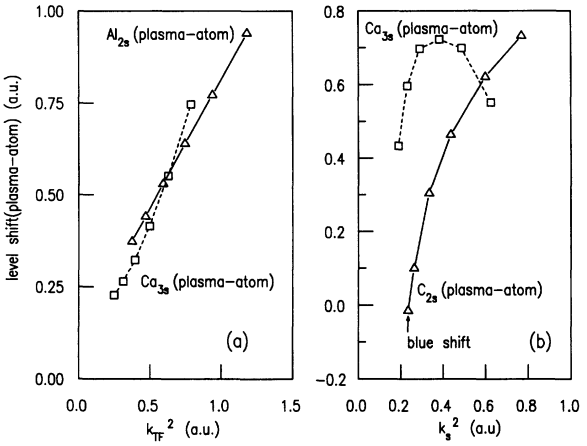

FIG. 3. (a) Energy shift $\Delta\varepsilon_i^{p-a}$ for $i=2s$ and $3s$ for Al and Ca ions in their plasmas (jellium model) as a function of the screening wave number $k_s^2=4/(\pi\alpha r_s)$ at zero temperature and as a function of the density. The Al density range is 5.7×10^{21} to 1.8×10^{23} electrons/cm^3. The Ca density range is 8.4×10^{20} to 5.4×10^{23} electrons/cm^3. (b) Energy shift $\Delta\varepsilon_i^{p-a}$ for $i=2s$ and $3s$ for Ca and C ions in their plasmas as a function of the screening wave number k_s^2 at fixed density and as a function of the temperature. The Ca and C densities are 2.7×10^{22} and 5.1×10^{23} electrons/cm^3, respectively, while the temperature range is $0.5T_F$ to $2T_F$ in both cases, where T_F is the Fermi temperature.

(i) Solutions that asymptotically tend to free-particle wave functions, i.e., phase-shifted spherical Bessel functions for $r>R_g$, the ion-correlation sphere radius [for $r>R_g$ the pair-correlation function $g_{ii}(r)$ is essentially unity]. These have energies $\varepsilon>0$.

(ii) Solutions that decay exponentially to zero within a length scale $r_a<r\le R_g$ and have energy $\varepsilon\le0$. Here r_a is the size of the plasma pseudoatom such that the electron density $n(r)$ is essentially that of the isolated atom (see Fig. 2). Note that r_a is $<r_{WS}$.

(iii) Solutions that decay exponentially to zero within a length scale $r\le r_a<r_{WS}$, and have energy $\varepsilon<0$.

The electrons of type (iii) are the core electrons, i.e., electrons essentially bound to the central ion. Let the number of these bound electrons per ion, obtained by integrating the density $n^b_{\text{core}}(r)$ defined by eigenstates of type (iii) alone, be n^b_{core}. The electrons of type (i) are not localized with respect to any nucleus; they are the free electrons n_f. The electrons of type (ii) are bound to the central ion and its *associated ion distribution.* The ion distribution actually consists of a time-evolving cluster of nuclei, and the electrons bound weakly to any ion in this dynamic cluster may be pictured as *hopping* among the quasilocalized states centered on each nucleus. We denote the number of such bound electrons per ion as $Z_{\text{hop}}=n^b_{\text{hop}}$. Since the cluster has been replaced by an average distribution, the KS eigenstates obtained for the average distribution represent the time-averaged envelopes of the transient multicenter eigenstates (hopping electron states) found in the plasma.

The effective charge Z^* to be ascribed to the central ion depends on energy scales and time scales. Since only electrons of type (iii) may be considered as true bound states associated with individual ions in the plasma, a strict definition would be to set $Z^*=Z-n^b_{\text{core}}$. The number of hopping electrons visiting any ion is given by

$$Z_{\text{hop}}=n^b_T-n^b_{\text{core}}\ , \tag{4.1}$$

where n^b_T is the total number of electrons in the bound spectrum of the DFT calculation [i.e., the sum of elec-

trons in categories (ii) and (iii)]. However, for certain physical processes some of the hopping electrons may behave as bound, while for others they may appear as free. This is particularly relevant to calculations of the frequency-dependent conductivity $\sigma(\omega)$ in a plasma. Further, the effective charge Z^* relevant to a given static process cannot always be identified with the global plasma neutrality parameter $\bar{Z}$ such that $\bar{n}=\bar{Z}\bar{\rho}$. Also, as seen from Table III, in many cases the estimate of $\bar{Z}$ depends significantly on how the ion distribution is modeled. Thus, in Table III, $\bar{Z}$ for the jellium model is 1.421, while that for the cavity model is 3.2470. Under such circumstances the NPA superposition assumption implicit in Eq. (2.9) that the cavity is a small perturbation on the energy levels is clearly inapplicable. [Also, standard AA models (e.g., HOPE, INFERNO) would yield incorrect values of Z^*]. Hence the coupled variation of both $n(r)$ and $\rho(r)$ implicit in the full DFT equations (2.4) and (2.5) becomes relevant. Then $\bar{Z}$ is found (in the column "profile" in Table III) to be ≈ 2.8.

In Chihara's [13] "quantal hypernetted-chain" approach to strongly coupled plasmas he defines an effective ionic charge $Z^*_{\text{Chihara}}=Z-n_T^b$, and hence ascribes *all* the bound electrons to the central nucleus. This may still be satisfactory at very low temperatures (e.g., in liquid metals) and for simple metallic systems (e.g., sodium, lithium, etc.). However, in hot plasmas the quasilocalized hopping extends over an energy range comparable to k_BT and Chihara's model, where Z^*_{Chihara} plays a central role in controlling bound-free interactions, etc., may lead to significant errors. Rozsnyai (see Ref. [9]) has recently calculated AA energy levels in an ion profile and divided the bound electrons n_T^b into a part $[1-g(r)]n_T^b$ ascribed to the central nucleus, and a part $g(r)n_T^b$ ascribed to the ion distribution. In calculating opacities he even partitions dipole matrix elements in the same manner. However, different eigenstates (e.g., ϕ_i and ϕ_j) have different extensions into the ion distribution and hence $\langle\phi_i|r|\phi_j\rangle$ cannot be meaningfully partitioned. The *ad hoc* division of n_T^b in terms of $g(r)$ is seen to be invalid if we consider the jellium limit where $g(r)=1$ for all r. Then, in Rozsnyai's model $[1-g(r)]n_T^b$ is zero and the central nucleus cannot be assigned any bound electrons, although an independent calculation with a jellium background establishes otherwise. Further, Rozsnyai treats the continuum electrons using a Thomas-Fermi model. Also, standard microfield methods assume a uniform neutralizing background, and cannot be used with AA models containing an ion profile to calculate opacities since ion-screening effects get over counted [25].

The delocalization of a bound state to become a free state when the density is increased does not induce discontinuities in the thermodynamic functions of the plasma [26]. However, it may be associated with the formation of resonant states that have positive energies ε, but a pronounced localized character (particularly for high l values) in some regions of space and an itinerant charge in other regions, as a result of tunneling. The existence of high peaks in the density of states reflects the existence of such levels, as illustrated in Fig. 4. Resonant

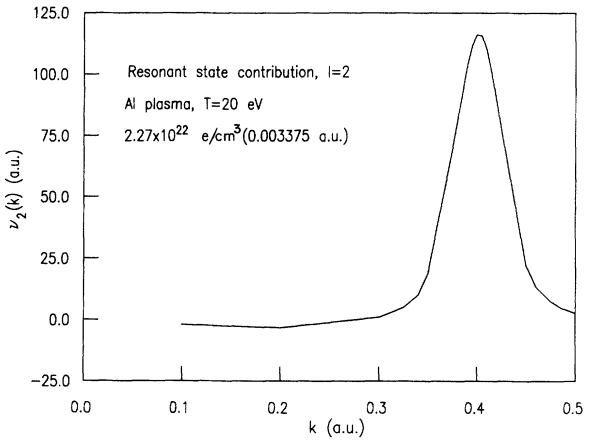

FIG. 4. Partial density of states $\nu_l(k)$ for the $l=2$ state showing resonant character for Al at 20 eV; the ion distribution is modeled as a cavity in jellium.

states contribute more or less to the ionization Z^*, and their effect on various properties may be difficult to analyze in simple models. At low temperatures they are responsible for the differences between simple metals and transition metals where the description of the total electron density as a superposition of pseudoatom densities break down. Fortunately, in general the importance of resonant states decreases with temperature.

Within this picture of hopping states in a transient ion distribution, the ionization of a bound electron in a plasma proceeds by the following steps: (i) the transfer of a bound electron to a hopping-electron state defined on a small part of the local cluster, (ii) transition of the electron to other (higher-energy) hopping states extending over a larger volume of the cluster, and (iii) eventual passage into the full delocalized, i.e., continuum states of the plasma, depending on the kinetic energy available to the ionizing electron. Thus the simple Saha picture (valid for nearly "ideal" plasmas) as a single-channel equilibrium of the form

(bound electrons)↔(free electrons)

has to be replaced by equilibria involving bound electrons, hopping electrons, and free electrons, via three channels [(bound)↔(hopping), (bound)↔(free), (hopping)↔(free)]. In fact, even in dilute plasmas, the ionization process probably proceeds via hopping states and not via the simple ionization process implicit in the Saha equation.

V. THEORY OF THE MOBILITY EDGE AND HOPPING STATES IN A PLASMA

The local cluster of ions defined by the $g(r)$ and higher correlation functions defines a disordered structure to which many of the ideas of electron localization and the formation of the mobility edge could be applied. If each ion center is called a *site,* Anderson's localization model treats the effect of variations in the on-site (or diagonal)

one-body potential as an electron hops from site to site, while the intersite interaction ("hopping" or "off-diagonal" matrix element) remains constant. In a plasma the hopping energy for electrons changes as the ions move to and fro. Hence off-diagonal disorder (the Lifshitz localization model) is also relevant in a plasma. The hopping is strongly controlled by whether a site is occupied or not. Hence the on-site Coulomb correlations ("Hubbard's U") central to the Mott mobility edge come into play. All these complicated effects control the density of states near the $\varepsilon=0$ energy region. The static (DFT) picture treats the hopping electrons and their eigenstates only in terms of the time- and angular-averaged envelope described by the $n^b_{\rm hop}(r)$ obtained from the DFT calculation. Explicitly multicentered Kohn-Sham codes are now available [27], but such calculations, using very limited basis sets, less than a hundred atoms, translationally invariant boundary conditions, etc., are not as trustworthy or as useful as conceptual models that reveal the physics of the process. Up to 30 ions are used by Younger *et al.* [28] and correspond to a cube of $\approx 3r_{\rm WS}$ along each side—thus the first peak of $g(r)_{ii}$ will not be fully treated, and no correlations beyond the first neighbor exist unless more ions are included. Also, as previously remarked [18], multicenter effects are not very pronounced in dense plasmas.

The DFT calculation with an ion profile $\rho(r)=\bar{\rho}g(r)$ provides us with the time-averaged and spherically averaged density $n^b_{\rm hop}$ of hopping electrons. The density of states $v(E)$ of these hopping states (i.e., prior to the averaging) fill up the energy "gap" between the last bound state of the ion and the nominal continuum edge whose position has been lowered due to (i) exchange-correlation effects of electrons and ions (by an amount $\Delta\mu$), as discussed in the context of Eq. (2.10a), and (ii) by the Friedel sum $\Delta\epsilon_{\rm FS}$ given as Eq. (2.10b). However, the "physical" onset of the continuum will be further changed due to the existence of the hopping density of states $v(E)$, where E is numerically a negative energy. There will be some energy E_m within the energy range of $v(E)$ such that states with $E>E_m$ will overlap sufficiently with other such states of neighboring transient clusters, forming a "percolation cluster" of infinite extent. Electrons in such energy states (i.e., $E>E_m$) can diffuse to infinity even though they are in localized states. Electrons in energy states, such that $E<E_m$, do not form an infinite percolation cluster and they remain localized for long times. The energy E_m is called the *mobility edge* and defines the physical onset of the continuum. Thus the energy of onset of the continuum can be given as

$$E_c=\Delta\mu+\Delta\epsilon_{\rm FS}+E_m \ , \tag{5.1}$$

The quantities on the right-hand side (5.1) are usually negative and hence they lead to a "lowering of the continuum." The theory of the density of localized states $v(E)$ as well as the associated mobility edge E_m is very complicated. Highly formal theories have been constructed, especially for zero-temperature systems with special restrictions on dimensionality (e.g., one-dimensional systems), interactions, etc. Here we use the basic ideas of the theory of disordered systems [14] and construct a simple model relevant to hot dense plasmas from which numerical estimates of E_m and $v(E)$ can be obtained. The results obtained from the present simple model [29] have been confirmed by more sophisticated techniques [30–32] (path-integral techniques, field theories, replica tricks, etc.). We assume the following model Hamiltonian:

$$H=H_0+H_1 \ , \tag{5.2}$$

$$H_0=(p^2/2m_e)+E_0 \ ,$$

$$H_1=\sum_i u(\mathbf{r}-\mathbf{r}_i)-U_0 \ . \tag{5.3}$$

H_0 is the kinetic-energy term of the hopping electron, and E_0 contains constants needed [cf., Eq. (5.1)] to define the energy zero. The potential $u(r-r_i)$ is the energy of interaction of an electron at r with an ion centered at $\mathbf{r}_i$. Hence $u(\mathbf{r}-\mathbf{r}_i)$ can be represented by a screened pseudopotential of the form

$$u(r)=-\frac{Z_c^*}{r+r_a}\exp(-k_{\rm SC}r) \tag{5.4}$$

where r is a radial distance and r_a the radius of the atomic core, already introduced in discussing $n^b_{\rm core}$. We can choose $k_{\rm SC}$ so that it, when used in linear-response theory (LRT), reproduces the free-electron density $\Delta n(r)$ obtained from DFT. This is not LRT and hence the previous symbol k_s [see Eq. (2.12b)] is not used for the screening wave vector. For strongly coupled plasmas $k_{\rm SC}\approx 1/R_g$ where R_g is the radius of the correlation sphere defined by $g(r)$ such that all its principle oscillations are contained within R_g and $g(R_g)\approx 1$. The mean energy U_0 occurring in (5.3) is the average potential given by integrating over the ion distribution, and is already treated in the DFT calculation.

Consider a cluster of p ions, in a volume ϑ, transiently occurring as a deviation from the normal density background. The lifetime of such a cluster is of the order of an ion-plasma oscillation that is long compared to electronic processes and hence H_1 of Eq. (5.3) applies. The potential fluctuation associated with the cluster is

$$U=(p-\bar{\rho}\vartheta)\int\frac{1}{\vartheta^2}u(\mathbf{r}_1-\mathbf{r}_2)d\mathbf{r}_1 d\mathbf{r}_2 \ , \tag{5.5}$$

where the integration is over the cluster volume ϑ. As in Friedberg and Luttinger [30], isoperimetric arguments could be invoked for considering ϑ to be spherical and having a radius r_ϑ. The kinetic energy of localization of an electron in ϑ is given by

$$E_\vartheta=(\pi^2/2r_\vartheta^2)\hbar^2/m_e \ . \tag{5.6a}$$

For large enough volumes ϑ, the distribution of levels for $E-U>E_\vartheta$ is quasicontinuous. A study of the dependence of E_ϑ and $v(E)$ by Chan, Louie, and Philips [29] on U for a variety of well shapes and models shows that there are three distinct regimes for the three-dimensional problem. These are where $\log v(E)$ is (i) Gaussian in $|E|$ for deep-lying levels, (ii) quasilinear in $|E|$ for a large

range of energies [30], and (iii) has a $|E|^{1/2}$ dependence in the Halperin-Lax [32] regime, for very small energies near the continuum edge. The free-particle distribution $v(E)$ behaves like $|E|^{1/2}$ and hence $\log v(E)$ falls into the quasilinear regime. We model the density of states for the given cluster in the spherical well as

$$v_c(E)=\begin{cases}(m_e^{3/2}\hbar^{-3})\pi^{-2}\vartheta[2(E-U)]^{1/2} & \text{for } E-U\geq fE_\vartheta \\ 0 & \text{for } E-U<fE_\vartheta\ .\end{cases} \tag{5.6b}$$

We use fE_ϑ as the cutoff where f will be chosen, following Kane [29], to normalize the distribution. The normalization condition (including a spin factor of 2) for $v_c(E)$ is

$$2\int_{-\infty}^{E_\vartheta} v_c(E)d(E-U)=1$$

and determines f to be 0.84. (A more systematic procedure is to numerically solve for the energy states of a spherical well given by the condition $\alpha\cot(\alpha r_\vartheta)=\beta$, where $\alpha=[2m(E-U)]]^{1/2}$, $\beta=[2m(-E)]^{1/2}$ and use the resulting distribution of energies. The present simple approach yields very similar results.)

For noninteracting particles, the Poisson distribution can be used for the probability of occurrence of a cluster of p ions in a volume ϑ. We have

$$P_0(p,\vartheta)=\frac{(\bar\rho\vartheta)^p}{p!}\exp(-\bar\rho\vartheta)\ . \tag{5.7}$$

For p interacting particles the interaction energy $E(p)_{\rm int}$, calculated as a sum of pair potentials constructed from the electron-ion pseudopotential of Eq. (5.4) has to be included via a Boltzmann factor of the form $A\exp[-\beta E(p)_{\rm int}]$. The constant A is determined from the normalization of $P(p,\vartheta)=P_0(p,\vartheta)A\exp[-\beta E(p)_{\rm int}]$. That is,

$$\sum_p P(p,\vartheta)=1\ . \tag{5.8}$$

The contribution to the density of states from all clusters requires a summation over p of $v(E)$ of each cluster weighted by $P(p,\vartheta)$. If the total volume is Ω there are Ω/ϑ cluster volumes that contribute. Converting the p summation to an integration, we have, for the whole plasma with volume Ω, on including the factor Ω/ϑ,

$$v(E)=(m_e^{3/2}\hbar^{-3})\Omega\pi^{-2}\int[2(E-U)]^{1/2}P(p,\vartheta)dp \qquad \text{for } E-U\geq fE_\vartheta\ . \tag{5.9}$$

The volume ϑ occurring in (5.9) is chosen so that the number of states below the nominal continuum edge [the zero of potential in H, Eq. (5.1)] is a maximum. That is, we require to choose the radius r_ϑ such that

$$N(0)=\int_{-\infty}^{0} v(E)dE \tag{5.10}$$

is maximized. The analysis can be easily carried through using $P_0(p,\vartheta)$. The probability factor $P_0(p,\vartheta)$ has its maximum value at $p=\bar\rho\vartheta$. Using Stirling's approximation for $p!$, and expanding about the average number of particles in the volume, viz., $\bar\rho\vartheta$, we obtain

$$P_0(p,\vartheta)\approx(2\pi\bar\rho\vartheta)^{-1/2}\exp[-(p-\bar\rho\vartheta)^2/2\bar\rho\vartheta]\ . \tag{5.11}$$

The fluctuation in the number of particles about the average $\bar\rho\vartheta$ is $p-\bar\rho\vartheta$. This quantity is significantly smaller than $\bar\rho\vartheta$, except in very dilute plasmas. Hence the approximation (5.11) is probably reliable for most plasma situations. Using (5.11) in (5.10) it can be shown that $N(0)$ has a *broad maximum* and for volumes ϑ such that $r_\vartheta\approx 0.7/k_{\rm SC}$. The broadness of the maximum implies that the numerical factor 0.7 is not too critical. Thus the optimal volume for considering particle fluctuations is of the order of a screening sphere. In the DFT model that is applicable to arbitrary couplings, the relevant volume is just that dictated by the range R_g of the pair distribution function $g(r)$, i.e., the correlation volume. Using this optimal volume, we have

$$(p-\bar\rho\vartheta)=U\Big/\int\frac{1}{\vartheta^2}u(r_1-r_2)dr_1dr_2\ .$$

Hence the probability distribution can be written in terms of U as

$$\begin{aligned}&P(U)=(2\pi N_0)^{-1/2}\exp(-U^2/2w)\ ,\\ &2w=N_0K^2,\quad N_0=\bar\rho\vartheta\ ,\\ &K=\int\frac{1}{\vartheta^2}u(r_1-r_2)dr_1dr_2\ .\end{aligned} \tag{5.12}$$

The constant N_0 is the number of particles in the optimal fluctuation volume ϑ (i.e., the volume of the correlation sphere). The fluctuations of the potential about the mean potential follow a Gaussian probability distribution with w playing the role of a variance. In this problem the (screened) Coulomb (SC) interactions are short ranged and the present result may be regarded as a manifestation of the central limit theorem, although we have not invoked it in our derivation. Using Eq. (5.12) in (5.9), the hopping electron density of states becomes

$$v(E)=(m_e^{3/2}\hbar^{-3})\Omega\pi^{-5/2}\eta\int_{-\infty}^{E}[2(E/\eta-z)]^{1/2}\times\exp(-z^2)dz\ , \tag{5.13}$$

$$\eta=(2w)^{1/2}=(2N_0)^{1/2}K_0\ . \tag{5.14}$$

The constant η defining the energy spread can be cast into a more transparent form if one notes that

$$K_0\approx e^2k_{\rm SC},\quad k_{\rm SC}r_\vartheta\approx 1 \tag{5.15}$$

for the choice of ϑ that maximizes $N(0)$ of Eq. (5.10).

This analysis does not recover the Halperin-Lax [32] regime close to the nominal continuum edge (this is a very narrow regime of energies and is probably unimportant to us). Energies very close to the continuum edge correspond to wave functions localized within a very large volume. Such "localized" states overlap with similar states whereby the electron diffuses through the whole plasma. As we move to more negative energies the localization of these states increases and we cross the mobility edge. We use a simple percolation argument to estimate the position of the mobility edge. The average length of

TABLE IV. Energies (in hartrees) relevant to the position of the bottom of the continuum in an Al-plasma. $\Delta\mu_{xc}$ and $\Delta\mu_{ie}$ denote shifts in the chemical potential due to electron exchange and correlation, and ion-electron correlation, respectively. E_{FS} is the contribution from the Friedel sum and E_m is the mobility edge correction. The electron density $\bar{n}=0.000\,843\,7$ a.u. corresponds to an $r_s=6.565$.

	$\bar{n}=0.0135$ a.u.		$\bar{n}=0.0008437$ a.u.	
	$T=T_F$	$T=2T_F$	$T=2T_F$	$T=4T_F$
μ	−0.005 649	−0.667 30	−0.104 61	−0.398 30
$\Delta\mu_{xc}$	−0.2619	−0.2301	−0.1106	−0.094 33
$\Delta\mu_{ie}$	−1.7048	−1.7309	−0.1077	−0.2845
$\Delta\varepsilon_{FS}$	0.1959	0.1072	0.0394	0.0201
E_m	0.1601	−1.0274	−0.0156	−0.6787
n^b_{core}	9.9982	9.7900	10.000	11.7486
$\bar{Z}$	2.2030	2.7969	0.4104	1.2545
Z_{hop}	1.0752	0.5288	3.0600	0.1774

any electron hop is $\sim r_{WS}$. An electron at the origin has to hop over a distance of about r_ϑ to hop out of the optimal volume ϑ. Since a random walk is involved, the required number of hops is estimated to be $N_{hop}=(r_\vartheta/r_{WS})^2$.

Since there are $N_0=\bar{\rho}\vartheta$ ions in the optimal well, the fraction of time occupied by an electron at any ion is N_{hop}/N_0. Since there are $Z_{hop}=n^b-n^b_{core}$ hopping electrons [see Eq. (4.1)] visiting each ion, the average population of electrons at the energy level that supports the required number of hops to diffuse out is given by

$$2/[\exp(E-\mu)\beta+1]=Z_{hop}N_{hop}/N_0\ , \tag{5.16}$$

where we have included a factor of 2 for spin. The energy E satisfying (5.16) is taken as the energy defining the mobility edge E_m. Using $N_{hop}=(r_\vartheta/r_{WS})^2$, $r_\vartheta k_{SC}\approx 1$ it is easy to show that

$$E_m=E=k_BT\ln[2/(Z_{hop}r_{WS}k_{SC})^{-1}-1]+\mu\ . \tag{5.17}$$

The final position of the lowered continuum is given by

$$E_c=\Delta\mu_{xc}+\Delta\mu_{ie}+\Delta\varepsilon_{FS}+E_m\ . \tag{5.18}$$

In Table IV we present data relevant to the calculation of the position of E_c as well as other quantities of interest. These calculations involve the solution of the Kohn-Sham equation for the electronic system, with the ion subsystem self-consistently coupled to give the profile $\bar{\rho}g(r)$. In the plasma at the density $\bar{n}=0.0135$ a.u. ($\frac{1}{2}$ the electron density in normal Al) and at a temperature $T=T_F$, the noninteracting chemical potential μ is nearly zero, and signals the passage from an essentially degenerate system to a nondegenerate system. The terms $\Delta\mu_{xc}(\bar{n})$ and $\Delta\mu_{ie}(\rho,\bar{n})$ were calculated as in Ref. [20]. That is, the distribution functions $g_{ee}(r)$ and $g_{ie}(r)$ are taken in the random-phase approximation. Both $\Delta\mu_{xc}(\bar{n})$ and $\Delta\mu_{ie}(\bar{\rho},\bar{n})$ contribute to a lowering of the continuum. The Friedel sum leads to a *raising of the continuum* for the four cases discussed here. The formation of a percolation cluster among the hopping electrons leads to the mobility edge term (or percolation contribution) E_m, and this is found to lower the bottom of the continuum, except in the plasma at $T=T_F$. In this plasma none of the hopping electrons can support a percolation cluster and suggests that all the hopping electrons are localized. Although the model is too simple to be definitive, the positive E_m may be interpreted as showing that a part of the bottom of the nominal continuum, up to 0.16 a.u., is also converted to localized (hopping) states. In the fourth and fifth columns we consider a plasma at $\frac{1}{32}$ of the normal Al density. Similar considerations (and caveats) apply to the $E_m=-0.0156$ entry in the fourth column where $\mu=-0.1046$ a.u. For calculating E_m we estimated k_{SC} as the reciprocal of the ion-cluster size dictated by the effective ion-ion coupling parameter Γ_{eff}. This is taken to be

$$\Gamma_{eff}=(\beta\bar{Z}^2/r_{WS})\exp(-k_sr_{WS})\ , \tag{5.19}$$

where k_s is the electron-screening wave vector of Eq. (2.12b). Then k_{SC} is defined via

$$k^2_{SC}=3\Gamma_{eff}/r_{WS} \tag{5.20}$$

and roughly corresponds to the reciprocal of the radius of the ion-correlation sphere.

The calculation of the density of states of hopping electrons in the region of the mobility edge includes thermal- and density-fluctuation-related disorder effects (approximately, Anderson- and Lifchitz-type localization mechanisms), but does not include the on-site Coulomb repulsion (Mott-Hubbard mechanism). The treatment of this disordered "Hubbard-model" problem is beyond the scope of this paper.

VI. SUMMARY AND CONCLUSION

We have studied the electronic states in plasmas as a function of the ionic and electronic environment of the plasma. Using density-fluctuation calculations, we concluded that ions in plasmas form "neutral pseudoatoms" with electron distributions closely approximating those of the isolated atoms. This clarifies why the plasma effect on energy levels is much smaller than that predicted by simple screening ideas, which do not account for orthogonalization of the continuum eigenstates to the core states, nonlinear effects, etc. The ionization process in a plasma is viewed as the progressive delocalization of an

electron via passage into hopping states and finally into the continuum. A compact expression for the density of hopping states is given. The ion-correlation sphere defined by the range of $g(r)$ is found to be the "optimal volume" containing the transient cluster that maximizes the number of hopping states supported by the plasma. The mobility edge is calculated via the statistically minimal number of hops required by the electron to diffuse out of the ion cluster. The continuum edge is shown to depend on the exchange and correlation effects of the ions and electrons, a Friedel-sum contribution, and a percolation contribution.

ACKNOWLEDGMENTS

This work was supported in part by the United States National Science Foundation under Grant No. PHY82-17853, supplemented by funds from the National Aeronautics and Space Administration at the University of California at Santa Barbara. A good part of this work was done during the "Atoms in Plasmas" workshop held at the institute of Theoretical Physics at Santa Barbara. We thank Jim Langer, the director of the Institute of Theoretical Physics at Santa Barbara, and the organizers of the "Atoms in Plasmas" Workshop, Joe Callaway, Hugh van Horn, and Hugh DeWitt, for the stimulating atmosphere that made this research possible. We also thank Walter Kohn, Neil Ashcroft, Hans Griem, Richard More, Dan Kelleher, and other participants for many stimulating discussions. The authors are particularly thankful to David Boercker for a very detailed critical reading and comments on a first version of the manuscript.

APPENDIX A: EXTENSION OF THE LINEAR-SCREENING EQUATIONS

The Coulomb interaction of the plasma electrons with the ith bound-state electron is contained in the last term of Eq. (3.4). This can be written as in Eq. (3.6),

$$\Delta\varepsilon_f^p = \langle V_{i,f}\Delta n_f^p \rangle \approx \int_0^\infty \Delta n_f^p(r')4\pi r'^2 dr'/r' \ .$$

The lower bound of the integration has been put to zero for simplicity. We start from the above equation and show how different shifts arise from details (of the dependence on the level i, screening and interactions) retained. The electron-gas response $\chi(q)$ in the random-phase approximation is

$$\chi(q)=\chi(q)^0/[1-V_q\chi(q)^0], \quad \chi(q)^0=-\frac{k_s^2}{4\pi}f^0(q) \ , \tag{A1}$$

where V_q is the Coulomb potential $4\pi/q^2$ and $f^0(q)$ contains the essential q dispersion. The density displacement is given to leading order in the ion-electron interaction $V_{ie}(q)$ by

$$\Delta n_f^p(q)=V_{ie}(q)\chi(q) \ . \tag{A2}$$

Let us consider different approximations to $V_{ie}(q)$ and $\chi(q)$ and the resulting energy shifts $\Delta\varepsilon_f^p$.

1. Debye-Hückel shift

Here the response function $\chi(q)$ is taken in the $q=0$ limit where $f^0(q=0)$ is unity. The electron-ion interaction is that of a point ion, viz., $V_{ie}(q)=-4\pi Z^*/q^2$. Then

$$\Delta\varepsilon_f^p=\frac{2}{\pi}k_s^2Z^*\int_0^\infty dq\frac{1}{(q^2+k_s^2)}=Z^*k_s \ , \tag{A3}$$

as in Eq. (2.13d). The shift is *independent* of the energy level i.

2. Ion with bound levels (pseudoatom)

Here the point ion is replaced by a point ion with structure and hence the electron-ion interaction is modeled as $V_{ie}(q)=-4\pi Z^*/(q^2+q_{ai}^2)$ where i is the level index and q_{ai} is of the order of the inverse atomic radius, i.e., $1/r_a$ pertinent to the shell i. Thus is $q_{ai}\gg k_s$. Hence in the small-q approximation for the response, we have, writing $q_{ai}=q_a$ for simplicity,

$$\Delta\varepsilon_f^p=\frac{2}{\pi}k_s^2Z^*\int_0^\infty\frac{q^2}{(q^2+q_a^2)(q^2+k_s^2)}dq$$
$$=Z^*k_s^2/(q_a+k_s)\approx Z^*k_s^2/q_a \ . \tag{A4}$$

Thus the shift is proportional to the square of the screening wave number and *strongly weakened* by the large $q_a=q_{ai}$. Even in this simple model there is a level dependence of the shift via q_{ai}.

3. Pseudoatom model inclusive of q dispersion

The small-q approximation is not justified for the response to a neutral pseudoatom, especially in the low-density regime. Let us consider the $T=0$ K case for simplicity. Then $\chi(q)^0=-(k_s^2/4\pi)f^0(q)$ can be written as $\chi(q)^0=-(k_F/\pi^2)f^0(\kappa)$ where $\kappa=q/k_F$, with $f^0(\kappa=0)=1$. Then the energy shift can be written as

$$\Delta\varepsilon_f^p=-\frac{2}{\pi^3}k_F\int_0^\infty d(k_F\kappa)V(k_F\kappa)\frac{f^0(\kappa)}{1+(k_s^2/\kappa^2k_F^2)f^0(\kappa)} \ .$$

Hence an upper bound to the shift is given by

$$|\Delta\varepsilon_f^p|\le\frac{2}{\pi^3}k_F^2|V(0)|\int_0^\infty d\kappa f^0(\kappa) \ . \tag{A5}$$

This integral converges since $f^0(\kappa)$ goes as $1/\kappa^2$ for large κ and $f^0(\kappa=0)=1$. Thus the use of the full q dispersion in $\chi(q)$ allows us to say that the shift decreases like k_F^2 (i.e., k_s^4), or even faster in the low-density case (Appendix B).

APPENDIX B: LOW-DENSITY REGIME

The dependence of the level shift on the square of the screening wave vector needs careful study for small densities (small k_s) since in Fig. 3 the level shifts do not extrapolate to zero as k_s goes to zero. From Figs. 3(a) and 3(b) it is clear that the $T=0$ case is simpler. At zero temperature $k_s^2=4/(\pi\alpha r_s)$, i.e., $4k_F/\pi$ and hence we use k_F to define the screening. In Fig. 5 we show the behavior of

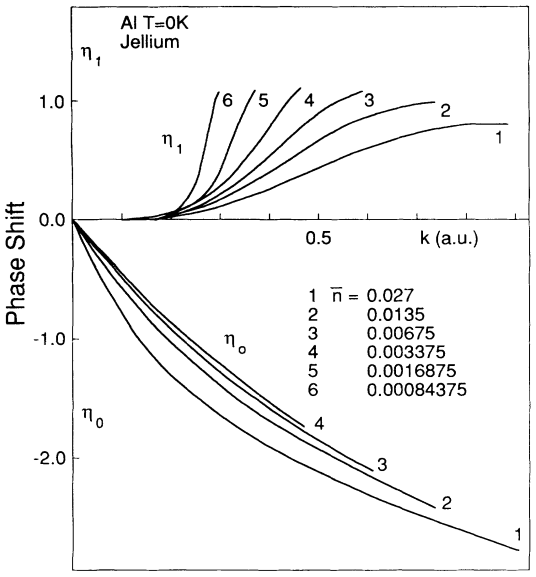

FIG. 5. The behavior of the s and p phase shifts η_0 and η_1 for Al in jellium at $T=0$ for a range of k values when the electron density is decreased.

the s and p phase shifts η_0 and η_1 for Al in jellium at $T=0$ for a range of k values when the electron density is decreased from normal density to $\frac{1}{32}$ of the normal density. η_0 converges towards a limit curve that corresponds to that obtained for the potential of the free atom with the configuration $3s^2 3p^1$. However, even for the lowest density displayed (curve 6), the p bound state has already ceased to exist. The change in η_1 is large and indicates the formation of a resonance in the continuum with an increase near the Fermi level, which becomes steeper and deeper for lower densities. As the phase shifts for $l \geq 2$ are negligible, the Friedel sum reduces to

$$Z_F \approx \frac{2}{\pi}[\eta_0(k_F)+3\eta_1(k_F)]=1 \ .$$

Now, because the $3s$ bound state exists, η_0 is negative, and hence η_1 must be positive and large to fulfill the sum rule. As the resonance can contain six electrons, the Fermi level must fall inside the resonance peak, showing that it is impossible for the resonance to go to zero energy (before the appearance of the $3p$ bound state) for a finite density (i.e., a finite k_F). In other words, the model cannot produce the $3p$ bound state of the free atom, and is not appropriate at the low-density limit. This is numerically manifested by convergence instabilities as the low densities are approached.

The situation is similar in C (configuration $2s^2 2p^2$). But in the case of Ca, where we have a closed-shell configuration $3s^2 3p^6 4s^2$, the bound state $4s$ exists down to vanishing electron densities. However, now there is a $3d$ resonance in the continuum that must stay above the Fermi level in order to satisfy the Friedel sum ($Z_F=0$). When the $3d$ resonance approaches the Fermi energy the instability develops.

When the plasma density is low enough, an atom in the plasma has most of the bound states of the free atom. The free-atom self-consistent potential $V_{\rm at}$ may then be an appropriate starting point for the calculation of the small screening effect in the plasma. Let the density induced (with no self-consistent adjustment of $V_{\rm at}$) by $V_{\rm at}$ in the electron gas be n_1. This may be easily calculated as the result of a single "iteration" in the DFT code, starting with $V_{\rm at}$. This n_1 consists of a bound and a free part, i.e., $n_1=n_{1b}+n_{1f}$. Even though $V_{\rm at}$ is "weak" in some sense, linear response cannot be applied directly to $V_{\rm at}$ since it supports many weak bound states. But it is reasonable to assume that the self-consistent free-electron density $n_{1f}^{\rm SC}$ is given by

$$n_f^{\rm SC}(q)=n_{1f}(q)/\epsilon(q)\approx V_{\rm at}\chi(q) \ ,$$

where $\epsilon(q)$ is the linear-response dielectric function. Then the perturbation correction due to $n_{1f}^{\rm SC}(q)$ on the low-lying bound levels is

$$\Delta\varepsilon_f^p \approx \int_0^\infty n_f^{\rm SC}(r)4\pi r^2 dr$$
$$\approx \frac{1}{(2\pi^2)}\int_0^\infty \frac{4\pi}{q^2} n_f^{\rm SC}(q)q^2 dq \ .$$

Now, writing $n_f^{\rm SC}(q)=V_{\rm at}\chi(q)$ and expressing q in units of k_F it is shown that $\Delta\varepsilon_f^p$ varies as k_F^2, i.e., as k_s^4, rather than linearly with k_F (i.e., as k_s^2). The above discussion is admittedly not rigorous but gives an indication of how the peculiarities of the low-density regime develop. It also highlights the importance of the Friedel-sum rule and casts doubt on those AA calculations that do not satisfy the sum rule.

*Electronic address: chandre@nrcvm01.bitnet; chandre@vm.nrc.ca.

†Permanent addresses of the authors.

[1] H. R. Griem, *Spectral Line Broadening in Plasmas* (Academic, New York, 1974); for other reviews, see S. Volonte, J. Phys. B **11**, 1615 (1978); J. Cooper, D. E. Kelleher, and R. W. Lee, in *Radiative Properties of Hot Dense Matter,* edited by J. Davis, C. Hooper, R. Lee, A. Merts, and B. Rozsnyai (World Scientific, Singapore, 1985); R. M. More, Adv. At. Mol. Phys. **21**, 305 (1985).

[2] M. W. C. Dharma-wardana, F. Grimaldi, A. LeCourt, and J-L. Pellisier, Phys. Rev. A **21**, 379 (1980).

[3] H. R. Griem, Phys. Rev. A **38**, 2943 (1988), and references therein.

[4] D. B. Boercker and C. A. Iglesias, Phys. Rev. A **30**, 2771 (1984). These authors have studied line shifts and not level shifts.

[5] H. Nguyen, M. Koenig, D. Benredjem, M. Caby, and G. Coulaud, Phys. Rev. A **33**, 1274 (1986); studies of two-center systems have been carried out by P. Malnoult, B. d'Etat, and H. Nguyen, Phys. Rev. A **40**, 1983 (1989); also D. Salzman, J. B. Stein, I. B. Goldberg, and R.H. Pratt,

ibid. **44**, 1270 (1991).

[6] For recent interest on partition functions, etc., see D. Mihalas, W. Dappen, D. G. Hummer, Astrophys. J. **331**, 815 (1988), and references therein.

[7] P. Hohenberg and W. Kohn, Phys. Rev. B **136**, 864 (1964); N. D. Mermin, Phys. Rev. A **137**, 1441 (1965); W. Kohn and L. J. Sham, *ibid.* **140**, 1133 (1965).

[8] M. W. C. Dharma-wardana and F. Perrot, Phys. Rev. A **26**, 2096 (1982); also *Strongly Coupled Plasmas,* edited by F. Rogers and H. E. DeWitt (Plenum, New York, 1986), p. 275; calculations using the Dyson equation for a plasma were given by the present authors in Phys. Rev. A **29**, 1378 (1984).

[9] B. F. Rozsnyai, Phys. Rev. **105**, 11 137 (1972); **20**, 1197 (1979); Phys. Rev. A **43**, 3035 (1991) attempts to use an ion distribution instead of the cell model, but the Thomas-Fermi continuum is still retained.

[10] See, for instance, G. Mahan, *Many-particle Physics* (Plenum, New York, 1983), Sec. 4.

[11] D. A. Liberman, Phys. Rev. B **20**, 4981 (1979).

[12] J. Davis and M. Blaha, J. Quant. Spectrosc. Radiat. Transfer **27**, 307 (1982).

[13] J. Chihara, Phys. Rev. A **33**, 2575 (1986), and references therein.

[14] See I. M. Lifshitz, S. A. Gredeskul, and L. A. Pastur, *Introduction to the Theory of Disordered Systems* (Wiley, New York, 1988).

[15] For a brief review of the band-tailing problem in amorphous systems, see M. H. Cohen, M. Y. Chou, E. N. Economou, S. John, and C. M. Soukoulis, IBM J. Res. Dev. **33**, 82 (1988).

[16] See J. M. Ziman, Proc. R. Soc. London **91**, 701 (1967); L. Dagens, J. Phys. C **5**, 2333 (1972); J. Phys. F **7**, 1167 (1977); F. Perrot, Phys. Rev. A **42**, 4871 (1990).

[17] The central ion is built up in detail but the "field ions" are treated approximately, as a continuum of point ions whose pseudopotential $\bar{Z}/r$ has a well radius equal to zero. A more elaborate pseudopotential constructed from the charge densities obtained at each iteration can be used [18]. For simplicity, here we use point ions with a charge $\bar{Z}$ for the ion distribution.

[18] M. W. C. Dharma-wardana and F. Perrot, Phys. Rev. Lett. **65**, 76 (1990), define pseudopotentials from charge densities. They also show that multicenter effects are negligible for the calculation of $S(k)$ and the electron density of states, as these agree with those from the quantum molecular-dynamics method of Car and Parinello [27], even in very dense plasmas like liquid Si at its melting point. See also M. W. C. Dharma-wardana, *Strongly Coupled Plasmas,* edited by S. Ichimaru (Elsevier/Yamada Science Foundation, Osaka, 1990), p. 409.

[19] Electron exchange-correlation potential V_{xc}^{e}, the electron-ion correlation potential V_{c}^{ei}, and the ion-ion correlation potential V_{c}^{i}. We shall sometimes use the notation $\Delta\mu_{xc}$, $\Delta\mu_{ei}$, $\Delta\mu_{ie}$, and $\Delta\mu_{ii}$ to denote these quantities calculated for a uniform system of electron density $\bar{n}$ and ion density $\bar{\rho}$. The possibility of evaluating these from the uniform system and making a connection to the chemical potentials arises because Kohn-Sham theory [7] shows that these potentials are universal functionals of the one-body distributions. Modeling [20] of the exchange-correlation effects using results from the uniform system requires the local-density approximation, where e.g., $V_{xc}[n(r)]$ is locally approximated by $V_{xc}[\bar{n}=n(r)]$ of the uniform system at $\bar{n}$. The LDA is found to be an excellent approximation even for rapidly varying density profiles due to favorable sum rules. For a general discussion of xc potentials and LDA, see *Theory of the Inhomogeneous Electron Gas,* edited by S. Lindqvist and N. H. March (Plenum, New York, 1983). Reference [20(b)] discusses some nonlocal xc potentials as well.

[20] (a) F. Perrot and M. W. C. Dharma-wardana, Phys. Rev. A **30**, 2619 (1984); (b) F. Perrot, Y. Furutani, and M. W. C. Dharma-wardana, *ibid.* **41**, 1096 (1990) for a modeling of different correlation potentials.

[21] W. D. Kraeft, D. Kremp, K. Kilimann, and H. E. DeWitt, Phys. Rev. A **42**, 2340 (1990). These authors conclude that electron-ion bound-state energies (i.e., levels) "may remain unshifted over a large density interval." We do not share this view (see Fig. 3). However, energies of spectral lines, which are to a first approximation a difference of a pair of level energies, can turn out to be only weakly dependent on the density, as may be ascertained from Eq. (3.6), from the discussion in the appendixes, or from detailed DFT calculations. This happens when the simple "linear" theory turns out to be adequate, as in the case of Fig. 3(a), but not for Fig. 3(b).

[22] L. A. Wolf and C. F. Hooper, Phys. Rev. A **38**, 4766 (1988). Here electron densities of 2×10^{23} cm^{-3} at temperatures of 1.1 keV for Be- and Li-like krypton have been studied. See also Woltz *et al.*, Phys. Rev. A **44**, 1281 (1991).

[23] X-Z. Yan and S. Ichimaru, Phys. Rev. A **34**, 2173 (1986); S. Tanaka and S. Ichimaru, in *Strongly Coupled Plasmas* (Ref. [18]), p. 545. See also S. Skupsky, Phys. Rev. A **21**, 1316 (1980).

[24] R. M. More, in *Atomic Physics of Highly Ionized Atoms,* edited by R. Marus (Plenum, New York, 1989).

[25] For microfield calculations that do not make the uniform background assumption, see F. Perrot and M. W. C. Dharma-wardana, Phys. Rev. A **41**, 3281 (1990); **33**, 3303 (1986).

[26] W. Kohn and C. Majumdar, Phys. Rev. A **138**, 1617 (1965).

[27] R. Car and M. Parinello, Phys. Rev. Lett. **55**, 2471 (1985).

[28] S. M. Younger, A. K. Harrison, K. Fujima, and D. Griswold, Phys. Rev. Lett. **61**, 962 (1988); S. M. Younger, A. K. Harrison, and G. Sukiyama, Phys. Rev. A **40**, 5256 (1989).

[29] E. O. Kane, Phys. Rev. **131**, 79 (1963); see also C. T. Chan, S. G. Louie, and J. C. Phillips, Phys. Rev. B **35**, 2744 (1987).

[30] R. Friedberg and J. M. Luttinger, Phys. Rev. B **12**, 4460 (1975).

[31] N. Bacalis, E. N. Economou, and M. H. Cohen, Phys. Rev. B **37**, 2714 (1988); S. John, M. Y. Chou, M. H. Cohen, and C. Soukoulis, *ibid.* **37**, 6963 (1988).

[32] B. I. Halperin and M. Lax, Phys. Rev. **148**, 722 (1966); see also J. Zittatrz and J. S. Langer, *ibid.* **148**, 741 (1966).